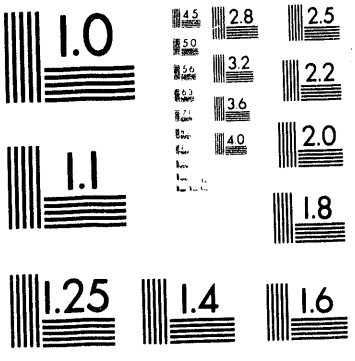
1.0
4.5
2.8
2.5
5.0
3.2
2.2
5.6
6.3
3.6
2.0
4.0
1.1
1.8
1.25
1.4
1.6

1 of 1

Conf-9309106--2

PNL-SA-22654

OXYGEN REDUCTION AT A YSZ INTERFACE WITH CATHODE MATERIALS $LA_{1-x}(CA\ OR\ SR)_xMNO_3$ OR $Y_{1-x}CA_xMNO_3$

G. E. Youngblood
C. F. Windisch Jr.
J. L. Bates

September 1993

Presented at the
14th Riso International Symposium on Materials Science: High Temperature Electrochemical Behavior of Fast Ion and Mixed Conductors
September 6-10, 1993

Work supported by
the U.S. Department of Energy
under Contract DE-AC06-76RLO 1830

Pacific Northwest Laboratory
Richland, Washington 99352

MASTER

OXYGEN REDUCTION AT A YSZ INTERFACE WITH CATHODE MATERIALS LA_{1-X}(CA OR SR)$_X$MNO$_3$ OR $Y_{1-X}CA_XMNO_3$

G.E. Youngblood, C.F. Windisch Jr. and J.L. Bates

Pacific Northwest Laboratory[1]
Richland, Washington, USA 99352

ABSTRACT

Impedance spectroscopy, in combination with an unbonded interface cell (UIC) design, was used to assess oxygen reduction behavior at an yttria-stabilized zirconia electrolyte interface with several substituted yttrium and lanthanum manganite cathode compositions. By analyzing the impedance spectra taken when using the UIC, the effective length of the reaction zone at the solid-gas triple phase boundary can be estimated and used to normalize the oxygen reduction reaction rate for each cell, thus effectively removing the influence of interface morphology. Intrinsic reaction rates (the specific oxygen activities) were determined from the spectra as a function of temperature and oxygen partial pressure for cathode compositions in the three systems La_{1-x}(Ca or Sr)$_x$MnO$_3$ and $Y_{1-x}Ca_xMnO_3$ (LC_xM, LS_xM and YC_xM, respectively) and for platinum.

The specific activities in the temperature and p(O_2) ranges of an operating solid oxide fuel cell (SOFC) cathode, 1173-1273K and 10^5-10^3 Pa, respectively, were highest for the LCM compositions, intermediate for the YCM compositions and lowest for the LSM compositions. For the LCM and YCM systems, compositions with x=0.5 gave the highest specific activities. The specific activities for all of the tested manganite compositions exceeded the platinum specific activities by at least an order of magnitude. In general, the shapes of the impedance spectra for all the manganite systems were similar. Detailed examination of the spectra shapes revealed that the overall cathodic polarization process was rather complex and made up of at least two or more fundamental steps.

1. INTRODUCTION

Hammouche, Siebert and Hammou (1989a) utilized pin-shaped electrodes abutted to a zirconia electrolyte disc to study oxygen reduction without the effects of morphology which are encountered when using porous electrodes. They determined the contact area of each pin electrode by using Newman's (1966) formula, $R_c = 1/4\sigma r$, to find the surface contact radius, r. In Newman's formula, R_c is the contact resistance and σ is

---

[1] Operated for the U. S. Department of Energy by Battelle Memorial Institute under contract DE-AC06-76RLO 1830.

the ionic conductivity of the electrolyte. Then Hammouche et al. (1989 a,b) calculated a specific current, equal to the measured current divided by $2\pi r$, to use in their analysis of dc polarization phenomena for several $La_{1-x}Sr_xMnO_3$ compositions. The use of a specific current eliminated the influence of morphology by assigning the generation of current to an effective reaction zone along the triple phase solid-gas boundary (tpb).

We have followed the same strategy except that our method uses impedance spectroscopy (IS) combined with an unbonded interface cell. With this method we determined the intrinsic oxygen reduction activities, independent of interface morphology, as a means to screen electrode compositions for use in SOFCs.

Others (Mizusaki, Tagawa, Tsuneyoshi and Sawata, 1989; Eguchi, Inoue, Ueda, Kamimae and Arai, 1991) have used the electrode conductance, σ_E, which is related to the electrochemical reaction kinetics; but σ_E itself depends upon the length of the tpb. Depending upon the interface preparation (cosintering, EVD, slurry-dip and sintering, screen printing, etc.) and upon operating conditions, the length of the tpb can vary by more than four orders of magnitude, e.g. 10^2-10^5 cm/cm^2. This makes comparison of different compositions difficult. Also, the morphology of a given electrode can change during testing or operation as has been pointed out by Copcutt and Maskell (1991).

In our method, the "effective reaction length" or the ERL, related to the length of the tpb, and the cathodic polarization resistance (R_p), are determined from a single IS scan. Then a specific activity (SA), a normalized reaction rate, is determined from:

$$SA = (ERL \times R_p)^{-1} \qquad (1).$$

With units of S/cm, SA is an intrinsic material property. In this study, SA was determined as a function of temperature, $p(O_2)$ and cathode composition. For a porous cathode with a typical ERL = 10^3 cm/cm^2 and for a cathodic polarization limited to 0.1 Ω-cm^2, Equation (1) also defines a useful "benchmark" SA value of 0.01 S/cm by which suitability of cathode compositions may be assessed.

2. EXPERIMENTAL PROCEDURE

The cathode materials tested were LC_xM (x=0.2 or 0.5), LS_xM (x=0.1 or 0.3), YC_xM (x=0.5, 0.6 and 0.7) and platinum. Manganite discs were pressed from powders and sintered to at least 90% of full density. Microstructural examination by SEM and XRD indicated the presence of only a single crystalline phase for each sintered disc. Small pellets (≈ 5 mm dia. x 2 mm thick), core-drilled from the discs, were mounted in the UIC configuration, which is depicted in Fig. 1.

In the UIC design, the sample pellet is pressed against a dense, yttria-stabilized zirconia (Tosoh TZ8Y) electrolyte disc. Mating surfaces were roughened by grinding with a 15 µm diamond wheel. Only about 10 to 20 actual electrical contacts occur between such surfaces. The counter and reference electrodes, on the backside of the 8YSZ electrolyte disc, were made from sintered platinum paste and mesh. Since the interface was unbonded, the cathode sample could be exchanged at the conclusion of each run without changing the 8YSZ electrolyte. The cell was mounted inside an

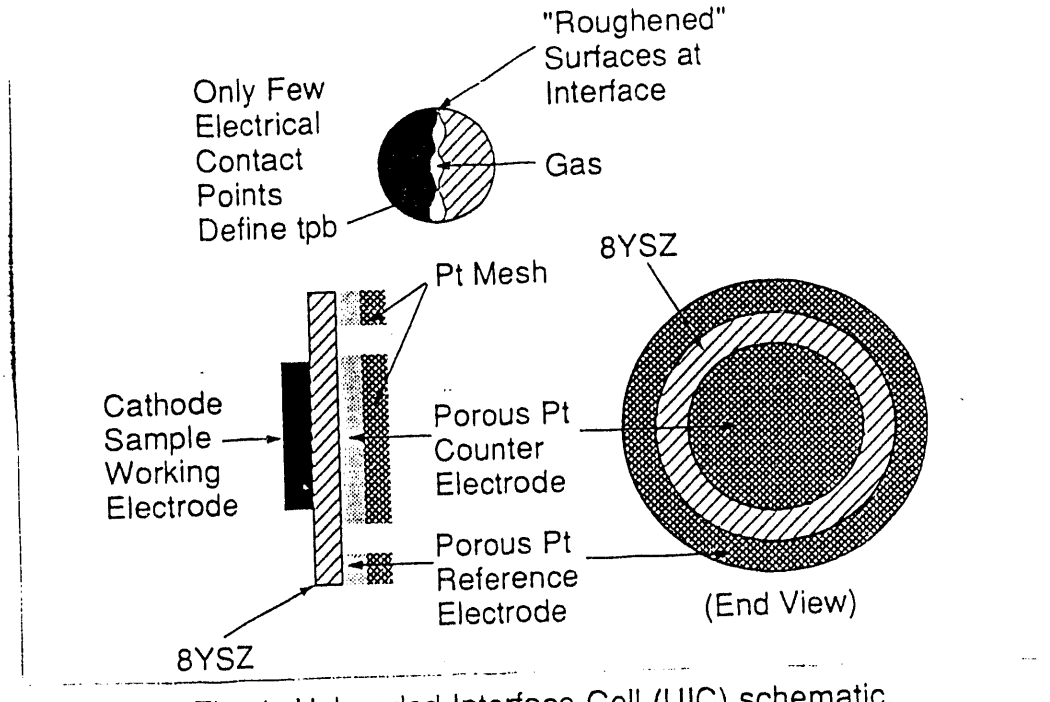

Fig. 1. Unbonded Interface Cell (UIC) schematic.

alumina tube in a furnace and heated in an appropriate flowing gas mixture (argon and air or oxygen). Complex impedance spectra were collected over a frequency range 0.6 Hz to 60 kHz. The IS data were analyzed using an equivalent electric circuit and the non-linear least squares fitting program EQUIVCRT (Boukamp, 1986).

3. EXPERIMENTAL RESULTS AND DISCUSSION

Typical Nyquist plots of the IS data taken at 1173K (900°C) for the YC_xM (x=0.6) sample are given in Fig. 2 for $p(O_2) = 10^5$, 10^4 and 10^3 Pa (1.0, 0.1 and 0.01 atm, respectively). The polarization curves appear to be composed of at least two arcs due to a higher (HF) and a lower (LF) frequency oxygen reduction process. With $p(O_2)$ =1.0 atm, the HF and the LF peaks have similar sizes; but the LF peak dominates the overall polarization more and more as the $p(O_2)$ is lowered. This also was the case as the temperature was lowered from 1173 to 973K.

Since the actual interfacial contact areas were relatively small for the UIC, R_c values (50 to 100 Ω at 1173K) dominated other ohmic resistances. In turn, ERL values fell within the 1-3 cm/cm^2 range. This range is very different from an ERL value for a typical, sintered porous electrode-electrolyte interface (10^3 cm/cm^2).

As an illustration of the typical behavior of the temperature and $p(O_2)$ dependence of the overall cathodic SA for manganites, values determined from IS data and Equ. (1) are shown in Fig. 3 for the LS_xM (x=0.3) sample. The temperature dependence for each $p(O_2)$ is indicated by assigning a psuedoactivation energy determined from the slopes for each straight line. For the LS3M sample, the straight lines are nearly parallel, and the psuedoactivation energies cover a narrow range from 1.29 -1.40 eV.

Single SA values for some LS_xM compositions (x=0.0, 0.1, 0.19, 0.3 and 0.5) in air at 960°C were estimated from the slopes at the origin of dc polarization curves given by

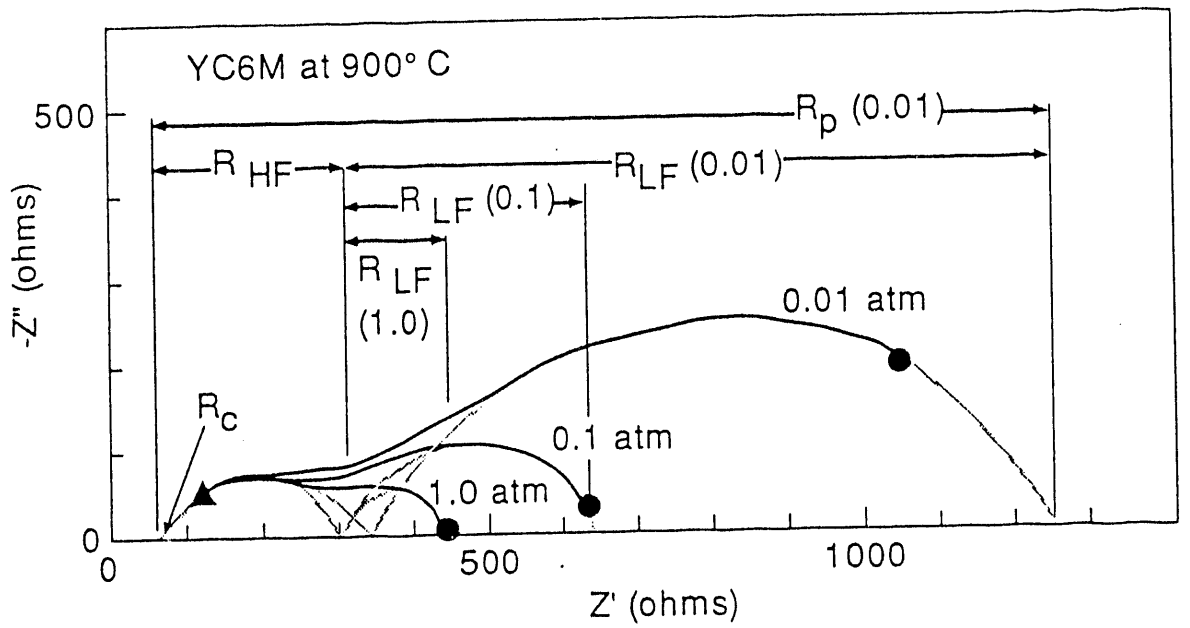

Fig. 2. $P(O_2)$ dependence of IS shapes for a YC_xM (x=0.6) cathode sample in a UIC at 1173K (900°C) when $p(O_2) = 10^5$, 10^4 and 10^3 Pa (1.0, 0.1 and 0.01 atm). The frequency range 60 kHz (Δ) to 1 Hz (•) is indicated. The high (low) frequency real axis arc intercept yields $R_c(R_p)$.

Hammouche et al (1989a). For comparison, these SA values are plotted onto Fig. 3 using dotted open square symbols. Relatively good correspondence is observed at 960°C for the SA value determined by our IS/UIC method and from Hammouche's data for the x=0.3 Sr composition.

As an overview, the temperature dependence of the overall SA values in air for the tested manganite materials is shown in Fig. 4. Except for LS1M above 1173K (900°C) the SA values determined for all other compositions exceeded the 0.01 S/cm benchmark. The SA values for the LCM and LSM systems increased with increasing dopant concentration, in accordance with the Hammouche LS_xM data in Fig. 3. All manganite SA values exceeded those for platinum by an order of magnitude or better. The SA values for LC5M, the highest measured, were about a factor of four higher than those for LS1M. Also, the lower pseudoactivation energies (slopes) determined for LC5M and LC2M (1.03 and 0.92 eV, respectively) lead to even a more pronounced advantage for these compositions below 1173K.

The $p(O_2)$ dependencies at 1173K (900°C) of the separated HF and LF process SA values for the LC_xM, LS3M and YC_xM materials are shown in Fig. 5. In the $p(O_2)$ range of 10^5 to 10^3 Pa (1.0 to 0.01 atm), the HF values are approximately independent of $p(O_2)$, while the LF values decrease as $p(O_2)$ decreases. The $p(O_2)$ dependence of the IS curves shown in Fig. 2 also indicate such a behavior. Assuming the LF process SA values vary as $p(O_2)^n$, the n-values would range from 0.1 to 0.9. For all the manganites, the rate determining step for the LF process appears to shift to control by molecular oxygen concentration as the $p(O_2) \approx 0.2$ atm (air) decreases to $\leq 10^{-2}$ atm. For the LS3M and YC_xM materials at 1173K in air, the cross-overs of the HF and LF lines indicate that the overall polarization (reciprocal of SA) would consist of at least two,

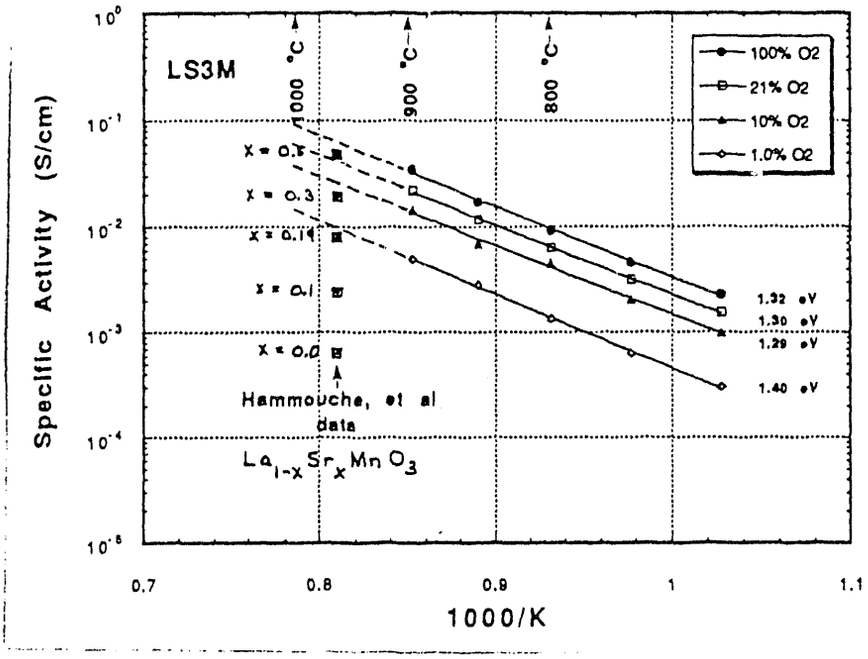

Fig. 3. Temperature and $p(O_2)$ dependence of the overall cathodic SA for the LS_xM (with x=0.3) sample. For comparison SA values estimated from dc polarization curves for LS_xM materials (x=0.0, 0.1, 0.19, 0.3 and 0.5) in air at 960°C by Hammouche et al (1989a) are indicated with a square box symbol.

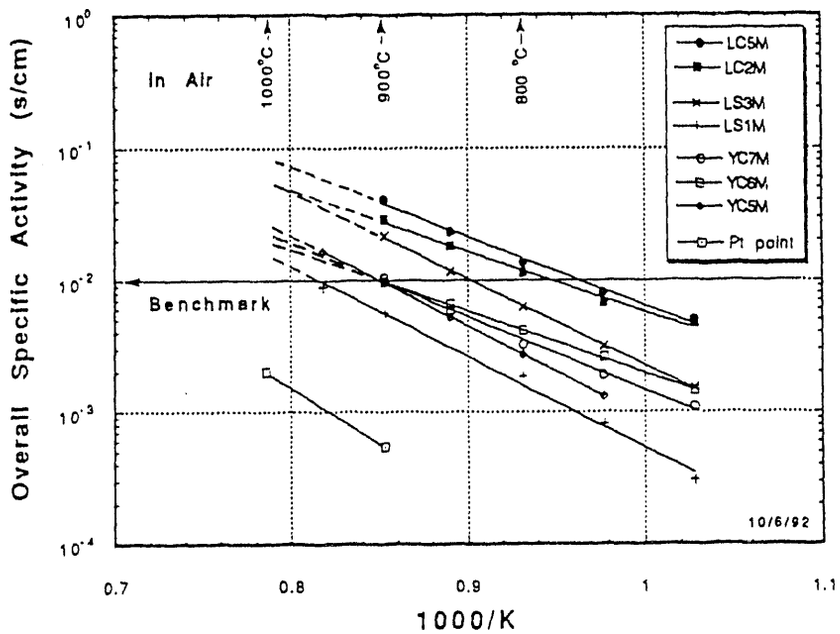

Fig. 4. Summary of the temperature dependence of the overall SA in air for several manganite cathodes (LS_xM, LC_xM and YC_xM) compared to that of platinum. A benchmark SA value of 0.01 S/cm, considered the minimum practical value for use as a cathode in a high-temperature SOFC, is indicated.

somewhat equivalent, HF and LF rate-limiting processes; while for the LC_xM materials, with high HF process SA values for all $p(O_2)$, the LF process would be rate-limiting.

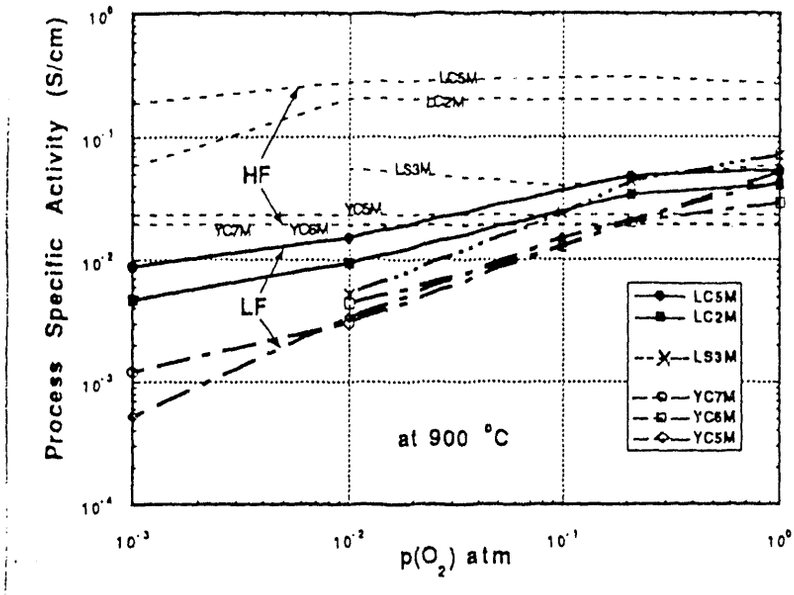

Fig. 5. The HF and LF process SA $p(O_2)$ dependence for the LC_xM (x=0.2 and 0.5); LS_xM (x=0.3) and YC_xM (x=0.5, 0.6 and 0.7) samples at 900°C.

ACKNOWLEDGMENTS

The authors gratefully acknowledge Dr. J. Stevenson, University of Missouri, Rolla, for providing the yttrium-calcium-manganite samples used in this study. The work was funded by the U. S. Department of Energy, Fossil Energy Materials Program.

REFERENCES

Boukamp, B.A. (1986). A nonlinear least squares fit procedure for analysis of immitance data of electrochemical systems. Solid State Ionics 20, 31-44.

Copcutt, R.C. and Maskell, W.C. (1992). CO/CO_2 electrochemistry on zirconia electrolyte with platinum electrodes in relation to amperometric oxygen sensors. Solid State Ionics 53-56, 119-125.

Eguchi, K., Inoue, T., Ueda, M., Kamimae, J. and Arai, H. (1991). The activation and transfer of oxygen at electrolyte/cathode interface for SOFCs. In: Proceedings of the second international symposium on solid oxide fuel cells. Edited by F. Grosz, P. Zegers, S.C. Singal and O. Yamamoto (The Commission of the European Communities, L-2920, Luxembourg) 697-704.

Hammouche, A., Siebert, E. and Hammou, A. (1989a). Crystallographic, thermal and electrochemical properties of the system $La_{1-x}Sr_xMnO_3$ for high temperature solid oxide fuel cells. Materials Research Bulletin 24, 367-380.

Hammouche, A., Siebert, E., Kleitz, M. and Hammou, A. (1989b). Oxygen reduction at the $La_{1-x}Sr_xMnO_3$/zirconia electrode. In: Proceedings of the first international symposium on solid oxide fuel cells. Edited by Subhash C. Singal (The Electrochemical Society, Inc., Pennington, NJ) 265-276.

Mizusaki, J., Tagawa, H., Tsuneyoshi, K. and Sawata, A. (1989). Reaction kinetics and microstructure of $La_{0.6}Ca_{0.4}MnO_3$/YSZ air electrode. In: Proceedings of the first international symposium on solid oxide fuel cells. Edited by Subhash C. Singal (The Electrochemical Society, Inc., Pennington, NJ) 254-264.

DATE FILMED

1 / 14 / 94

END